Journal of the Energy Institute 119 (2025) 101995

Contents lists available at ScienceDirect

Journal of the Energy Institute

journal homepage: www.elsevier.com/locate/joei

Influence of oxygen equivalence ratio on biochar oxidation characteristics under biomass oxidative pyrolysis conditions in a fluidized-bed reactor

Tianyu Lu [a,b], Dan Lin [a], Yusuf Makarfi Isa [c], Alexander Kozlov [d], Maxim Penzik [d], Xing Xie [a,**], Shihong Zhang [e], Haiping Yang [e], Bin Li [a,b,*]

[a] School of Energy and Power Engineering, Jiangsu University, Zhenjiang, 212013, China
[b] School of Engineering, Anhui Agricultural University, Hefei, 230036, China
[c] School of Chemical and Metallurgical Engineering, University of the Witwatersrand, Johannesburg, 2050, South Africa
[d] Melentiev Energy Systems Institute SB RAS, 130 Lermontov Street, Irkutsk, 664033, Russia
[e] State Key Laboratory of Coal Combustion, School of Energy and Power Engineering, Huazhong University of Science and Technology, Wuhan, 430074, China

ARTICLE INFO

Handling Editor: Paul Williams

Keywords:
Biochar oxidation
Low-oxygen concentration
Oxygen equivalence ratio
Fluidized-bed reactor
Physicochemical structure

ABSTRACT

The effect of oxygen equivalence ratio (ER of 0–9.83 %, corresponding to O_2 concentration of 0–3%) on biochar oxidation characteristics under oxidative pyrolysis conditions was investigated in a quartz-tube fluidized-bed reactor. The results showed that under lower ERs and 600 °C, there were two competing oxidation reactions between biochar and oxygen to respectively form CO and CO_2, resulting in insignificant changes in biochar oxidation consumption when ER increasing in the range of 1.65–4.94 %. When ER was below 2.29 %, the contents of CO and CO_2 both increased rapidly. With ER Further increasing, oxidation of biochar tended to produce more CO_2, which was favorable for reducing the biochar oxidation consumption and releasing more heat during oxidative pyrolysis of biomass. When ER was of 4.94 %, the content of CO_2 in the produced gas exceeded that of CO. Under low-oxygen concentration (low ER) conditions, the oxidation of biochar tended to consume the combustible C and H in biochar, whereas the O content in biochar was observed to increase. The oxidation etching of biochar also introduced more micropores on the char surface, and altered its surface chemical structures to form more oxygen-containing functional groups. The hydroxyl (-OH) group improved significantly, and the aromatization degree of biochar also increased. The results reported in the study show the prospect to directly obtain optimized structures of active biochar from oxidative pyrolysis of biomass by simply adjusting the oxygen concentration/equivalence ratio.

1. Introduction

Biomass is an important net-zero emission renewable resource, its efficient utilization at a large scale is a key solution for the future global carbon neutrality at 2050 [1]. Pyrolysis of biomass is one of the promising ways to efficiently convert biomass into value-added products, including combustible gas, liquid bio-oil and solid biochar [2,3]. Pyrolysis of biomass is usually carried out in an oxygen-free/inert atmosphere at moderate temperatures. It is an endothermic reaction process, an external heat supply is often required to sustain the pyrolysis reaction [4,5]. The pyrolyzer is normally heated through its surface. When scaling up a pyrolysis technology, the pyrolyzer would be only scaled up as its surface according to the heat transfer principle, not as its volume, resulting in reduced volumetric efficiency and increased cost of per unit processing capacity [6,7]. The rapid and efficient supply of a large amount of external heat to the pyrolyzer becomes a crucial bottleneck issue to be overcome.

Oxidative pyrolysis of biomass is a recently developed novel pyrolysis technology to overcome the heat supply issue during scaling up [8,9]. A small amount of oxygen with equivalence ratio (ER) generally <10 % is introduced into the pyrolysis process. The partial oxidation of biomass pyrolysis products in situ provides the heat demand for the endothermic reactions during pyrolysis process [10]. Autothermal pyrolysis is thus achieved for oxidative pyrolysis of biomass [11–13]. Oxidative pyrolysis of biomass changes the heat transfer mode of pyrolyzer from traditional surface heating to volumetric heating, thus

* Corresponding author. School of Energy and Power Engineering, Jiangsu University, Zhenjiang, 212013, China.
** Corresponding author.
E-mail addresses: xiexing_xx@126.com (X. Xie), libin198520@126.com (B. Li).

https://doi.org/10.1016/j.joei.2025.101995
Received 10 December 2024; Received in revised form 7 January 2025; Accepted 8 January 2025
Available online 9 January 2025

realizes that the pyrolyzer can be now scaled as its volume, the volumetric efficiency of the pyrolyzer after scaling up can be largely improved compared to that for non-oxidative pyrolysis of biomass, showing a very good application prospect [9].

The introduction of oxygen into pyrolysis process will definitely oxidize or consume some of the substances, thus affecting the final composition, distribution and physicochemical structures of the pyrolysis products [14–17]. Li et al. [10] found that oxidative fast pyrolysis of dried sawdust achieved autothermal operation at an ER of ~4 %, and the oxidation of biochar provided the main heat demand for the pyrolysis process. Biochar is a carbon-rich solid material which is usually produced by pyrolysis of biomass in an oxygen-free/inert atmosphere [18]. It can be used as a green fuel to replace traditional fossil fuels, significantly reducing the environmental pollution and carbon emissions. Meanwhile, biochar also shows great potential for applications in energy storage, catalytic materials, adsorption and gas separation [9]. For instance, the biochar was reported to achieve a good adsorption of organic pollutants (e.g., tetracycline and toluene) by surface modification [6,19]. Compared to traditional non-oxidative pyrolysis, oxidative pyrolysis of biomass has not yet been sufficiently investigated. Although some studies have been carried out to investigate the effects of oxygen concentration and temperature on the pyrolysis process [20], the physicochemical properties of biochar and its oxidation mechanism under oxidative pyrolysis conditions are still unclear.

The biochar surface usually contains a large amount of amorphous carbon and oxygen-containing functional groups, which can be served as active adsorption sites for oxygen molecules. Under low-concentration oxygen and lower temperature, the formation of gas products from the oxidation of nascent char is closely related to the active sites on char surface, and the existing forms and characteristics of the chemisorption intermediates/precursors [21]. Amutio et al. [13] analyzed the gas products of oxidative fast pyrolysis of biomass and found that at 500 °C with the increase of oxygen concentration (or ER), the CO_2 content in the produced gas increased dramatically, but the CO content changed insignificantly; a similar finding was also reported by Polin et al. [22]. In addition, the biochar oxidation conditions, such as oxygen concentration, reaction temperature, reaction time, etc., all have significant influences on the physicochemical properties of biochar [11,13,23]. Xiao et al. [24] conducted hot air oxidation of biochar at 300–700 °C, it was found that the air oxidation of biochar at higher temperatures would significantly increase its surface area and porosity, as well as the adsorption capability for neutral organic substances. Suliman et al. [25] found that the biochar prepared at lower temperatures was more susceptible to be oxidized, and the oxidation process might result in a slight decrease or increase in microporous volume and surface area. In addition, during oxidative pyrolysis of biomass, the physical structure and the surface active sites of biochar would change dynamically along with the oxidation etching of biochar surface by oxygen molecules, and such changes further affect the oxidation reactivity and final use of biochar [26,27]. Unfortunately, very few studies focus on the oxidation of biochar during oxidative pyrolysis of biomass at present, the oxidation characteristics and the structure evolution of biochar under such low-concentration oxygen atmosphere and pyrolysis temperature range are still rarely reported.

Therefore, in this study, the oxidation characteristics of biochar under oxidative pyrolysis conditions were investigated. To avoid the influence of volatiles oxidation during the oxidative pyrolysis of biomass, the biochar was firstly prepared under an inert atmosphere, and then the biochar oxidation experiments were directly carried out in a quartz-tube fluidized-bed reactor under various oxygen ERs. The oxidation characteristics and evolution of physicochemical structures of biochar were analyzed in-depth. The results of this study will not only help to understand the oxidation characteristics of biochar in low-concentration oxygen atmosphere, but also provide insights into the mechanism of selective oxidation of biochar under oxidative pyrolysis conditions.

2. Experimental

2.1. Materials

The biochar used in the study was prepared from the pyrolysis of pine sawdust. The pine sawdust was dried before pyrolysis, with a particle size of 90–180 μm. It was pyrolyzed in a horizontal tube furnace at 600 °C for 30 min under an N_2 atmosphere of 500 mL/min. The biochar preparation process showed good stability with the biochar yield of 20.04 wt% ± 0.40 wt%. The composition of the biochar was as follows: 90.74 wt% C, 2.71 wt% H, 5.80 wt% O, 0.16 wt% N, and 0.59 wt% ash.

2.2. Experimental setup and methods

The biochar oxidation experiments were carried out in a quartz-tube fluidized bed reactor, as shown in Fig. 1. The whole reaction system consisted of a mixed gas supply system, a conical quartz-tube fluidized bed reactor heated with electric furnace, a gas cleaning unit and a gas collection bag. The quartz-tube ($\delta = 1$ mm) fluidized bed reactor consisted of a bottom cone section with the OD of 10 and 40 mm and a height of 75 mm, and an upper column section with an OD of 40 mm and a height of 40 mm.

For each experiment, 0.5 g of biochar was accurately weighed and loaded into the reactor in advance. The inlet/fluidizing gas was a mixture of N_2 and air, with a total flow rate of 300 mL/min. Pre-experiments showed that the fluidization of the biochar inside the reactor was good with such gas flow rate at the reaction temperature (600 °C). The oxygen concentration of the mixed gas was regulated by two separated mass flow controllers. It was controlled at 0, 0.5 %, 0.7 %, 1.0 %, 1.5 %, 2.0 %, 2.5 %, and 3.0 %, corresponding to the ER (calculated using the experiment time scale of 10 min) of 0, 1.65 %, 2.29 %, 3.28 %, 4.94 %, 6.59 %, 8.26 %, and 9.83 %, respectively. The oxidation reaction temperature was controlled by the electric furnace and kept constant at 600 °C. The reactor was quickly placed into the constant temperature zone of the electric furnace, and the biochar was fluidized by the oxygen-containing mixture gas, heated rapidly and oxidized. The gas residence time inside the reactor was calculated as around 5.75 s. The resulted gas was condensed and scrubbed, and finally collected by a gas bag for further analysis.

Each experiment lasted for 10 min. After the experiment finished, the gas bag was immediately closed and removed from the system. The air flow was turned off, and the quartz-tube fluidized-bed reactor was quickly taken out from the furnace and rapidly quenched in an N_2 atmosphere. After cooling down to room temperature, the N_2 flow was turned off, and all the pipelines connected with the reactor were removed. The weight of the reactor with biochar was taken by an analytical balance before and after reaction. The remained biochar after reaction was finally collected in a sample bottle with a closed cap and stored in a desiccator for further analysis. Repeated experiments were done to confirm the reproducibility of the results. The average results with the standard deviations were finally presented in the study. To simplify the name of the biochar samples, the ER used during the experiment was also directly termed as the biochar sample after oxidation.

2.3. Product characterization and analyses

2.3.1. Characterization of gaseous products

The gaseous products generated from the oxidation of biochar were analyzed with a gas chromatograph (GC-9790II, Zhejiang Fuli Analytical Instruments Co., Ltd.) equipped with TCD and FID detectors. The main gas components detected were H_2, CO, CO_2, CH_4, and C_{2+} (i.e., C_2H_4, C_2H_6, C_3H_6, and C_3H_8), and the detailed information and operation procedure of the GC can be found in Refs. [28–30]. The GC was calibrated using a standard gas before the test. The gas composition was

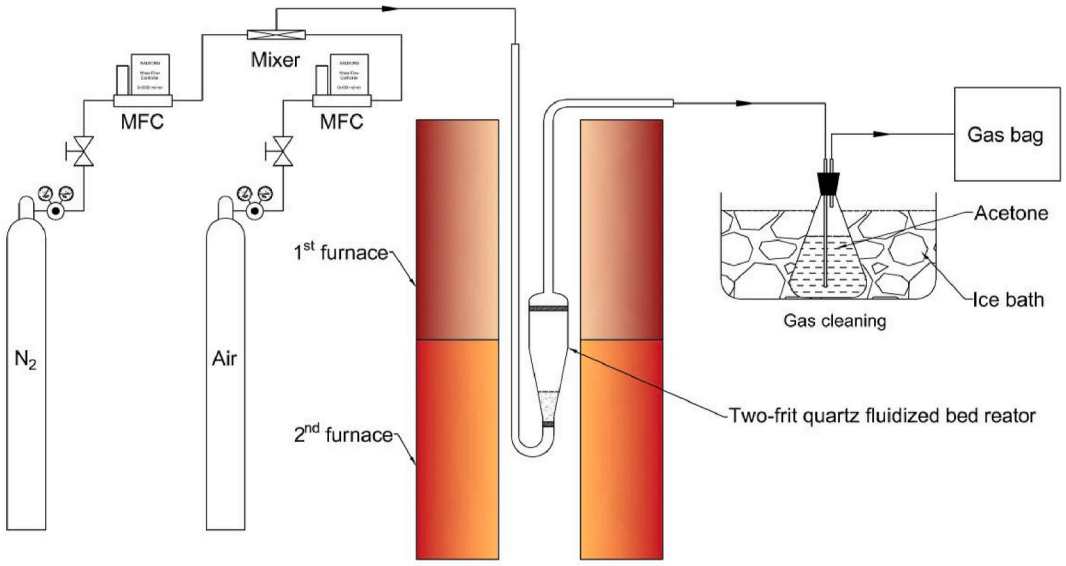

Fig. 1. A quartz-tube fluidized bed reaction system for biochar oxidation.

thus obtained through the external standard method. The gas yield was calculated by N_2 balance. Specifically, the total volume of N_2 in the gaseous product was known. For instance, with oxygen concentration in the inlet gas of 0, the total volume of N_2 could be calculated as 300 mL/min × 10 min = 3000 mL. The concentration of N_2 in the gaseous products was obtained from the GC test, so that the volume of the gaseous product (including N_2) could be calculated as (3000 ÷ N_2 concentration) mL. The final gaseous product (N_2 free) could be thus obtained by the above result minus the N_2 volume.

2.3.2. Characterization of biochar before and after oxidation reaction

The weight loss of biochar before and after oxidation reaction was determined by the weight difference of reactor (with biochar inside) before and after reaction.

The elemental composition (C/H/N/S) of biochar was analyzed using an elemental analyzer (Elemantar Vario EL cube, Germany). The ash content of biochar was determined using a muffle furnace for biochar burning at 550 °C for 3 h accordingly to the national standard GB/T 36057-2018 [31]. The O content of biochar was finally calculated by difference.

The microporosity of biochar was determined by N_2 adsorption-desorption method (Micromeritics ASAP 2020 M). Each sample was degassed at 200 °C for 6 h before test to remove any impurities adsorbed on the sample surface. The specific surface area of biochar was calculated using the Brunauer-Emmett-Teller (BET) method, and the pore size distribution of biochar was analyzed using the Barrett-Joyner-Halenda (BJH) and t-Plot methods [32].

The surface functional groups of biochar were determined by Fourier transform infrared (FTIR, Nicolet 5700) spectrometer. KBr tablet method was used during the test, where the biochar and spectroscopically pure KBr were thoroughly ground and mixed in a mass ratio of 1:300 and pressed into a tablet for analysis. The testing spectral range of the FTIR was of 4000-400 cm^{-1} with a resolution of 4 cm^{-1} and a cumulative total of 32 scans [33].

3. Results and discussion

3.1. Weight loss of biochar after oxidation reaction under lower oxygen ERs

Considering that oxidative pyrolysis of biomass is usually carried out at lower oxygen ERs (<10 %), the oxidation of biochar under oxidative pyrolysis conditions also used lower oxygen ERs in this study. Eight oxygen ERs of 0, 1.65 %, 2.29 %, 3.28 %, 4.94 %, 6.59 %, 8.26 %, and 9.83 % were selected during the experiments, corresponding to the oxygen concentrations in the inlet mixture gas of 0, 0.5 %, 0.7 %, 1.0 %, 1.5 %, 2.0 %, 2.5 %, and 3.0 %, respectively. Fig. 2 shows the effect of oxygen ERs on the weight loss rate of biochar after oxidation reaction in a quartz-tube fluidized-bed reactor at 600 °C.

As can be seen from Fig. 2, under an oxygen-free atmosphere (ER = 0), the biochar still gained some weight loss of 7.13 wt% when heat treated at 600 °C. It might be attributed to the further releasing of volatiles and moisture in biochar. After introduction of oxygen, with ER increasing, the oxidation consumption of biochar generally increased its weight loss rate. At an ER of 9.83 %, the weight loss rate of biochar increased to 19.06 wt% within 10 min oxidation at 600 °C. It should be noted that at lower ERs of 1.65%–4.94 %, the increase of ER did not lead to a significant increase in the oxidation consumption of biochar. This might be related to the fact that the oxygen concentration in the inlet mixture gas was very low, of only 0.5–1.5 %, and the oxidation of

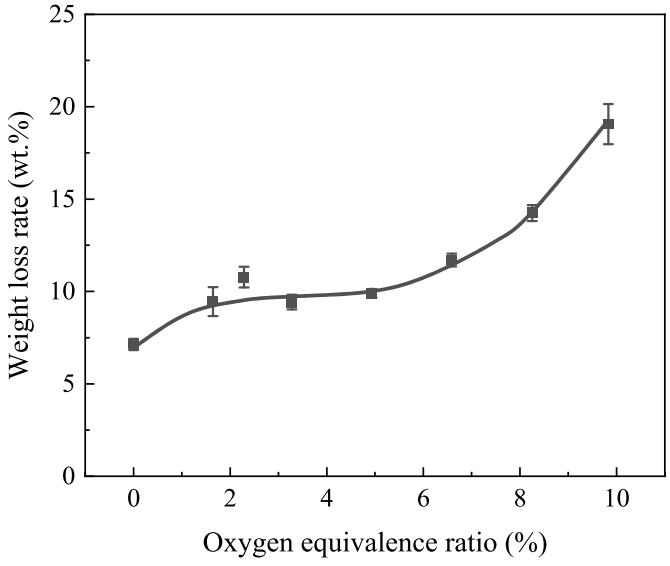

Fig. 2. Weight loss rate of biochar after oxidation reaction in a quartz-tube fluidized-bed reactor under different oxygen ERs at 600 °C.

biochar was actually carried out in an oxygen-deficient atmosphere (low ERs). There were two competing oxidation reactions, for which 1 atom of C would react with 0.5 O_2 to form CO or react with 1 O_2 to form CO_2, simultaneously. In this case, the increase of ER in the above range might result in insignificant oxidation consumption of biochar.

3.2. Gaseous products from biochar oxidation under lower oxygen ERs

The composition and distribution of gaseous products would somehow reflect the possible chemical reactions occurring during biochar oxidation under oxidative pyrolysis conditions. Fig. 3 shows the product gas composition and volumetric yield from biochar oxidation in a fluidized-bed reactor under different oxygen ERs at 600 °C.

As can be seen from Fig. 3 (a), under an oxygen-free/inert atmosphere (ER of 0), the heat treatment of biochar at 600 °C could further release a certain amount of small molecule gases such as H_2, CO, CO_2 and CH_4, indicating the occurrence of further dehydrocondensation, deoxygenation (i.e., decarbonylation and decarboxylation), and cleavage of hydrocarbon side chains. After introduction of oxygen, the concentrations of H_2, CH_4 and C_{2+} decreased significantly. The introduced oxygen reacting with combustible H_2 and hydrocarbon gases might be a possible reason leading to their consumption. In addition, it might be also attributed to the direct oxidation of H and hydrocarbon side chains on the biochar surface to form H_2O and CO_X gases under the oxidative pyrolysis atmosphere. In contrast, the concentrations of CO and CO_2 increased dramatically, mainly due to the oxidation of C in the biochar. The CO concentration peaked at 47.27 vol% at an ER of 2.29 % and then gradually declined with ER further increasing, while the CO_2 concentration continued to rise. This further indicated that under lower ER (oxygen concentration), the biochar surface would compete for oxygen to form CO and CO_2, respectively. With ER below 2.29 %, the concentrations of CO and CO_2 both increased rapidly, but further increasing ER, the biochar oxidation tended to generate more CO_2. The concentration of CO_2 in the product gas exceeded that of CO at an ER of 4.94 %. Further increasing ER could continue to increase the concentration of CO_2 but decrease the concentration of CO. This trend could be also corroborated by Fig. 2, as the insignificant changes in weight loss rate of biochar after oxidation reaction in the ER range of 2.29–4.94 % were observed due to the possible competing oxidation reactions. It is important to point out that the formation of more CO_2 during biochar oxidation at a relatively higher ER is more favorable for oxidative pyrolysis of biomass, as more heat would be released to meet the heat demand for biomass pyrolysis with relatively less consumption of biochar.

From the volumetric yield results of gaseous products in Fig. 3 (b), it can be seen that with ER increasing, the total gas yield increased rapidly due to more oxygen introduced into the biochar oxidation process to facilitate the formation of gaseous products. However, it was also observed that the yields of H_2, CH_4, and C_{2+} decreased continuously, which was consistent with the foregoing analysis, the increase of oxygen would result in their consumption or direct oxidation of their precursors in biochar to inhibit their formation. Moreover, the increase of ER tended to oxidize more C in biochar to form CO and CO_2. From Fig. 3 (b), it can be also found that at ER of 2.29 % and above, the increasing rate of CO_2 yield in the gaseous products was obviously higher than that of CO yield, directly causing the increase of CO_2 concentration and the decrease of CO concentration. Higher oxygen ER (or concentration) was favorable for the more sufficient oxidation of biochar to generate more CO_2, which was beneficial to the oxidative pyrolysis of biomass.

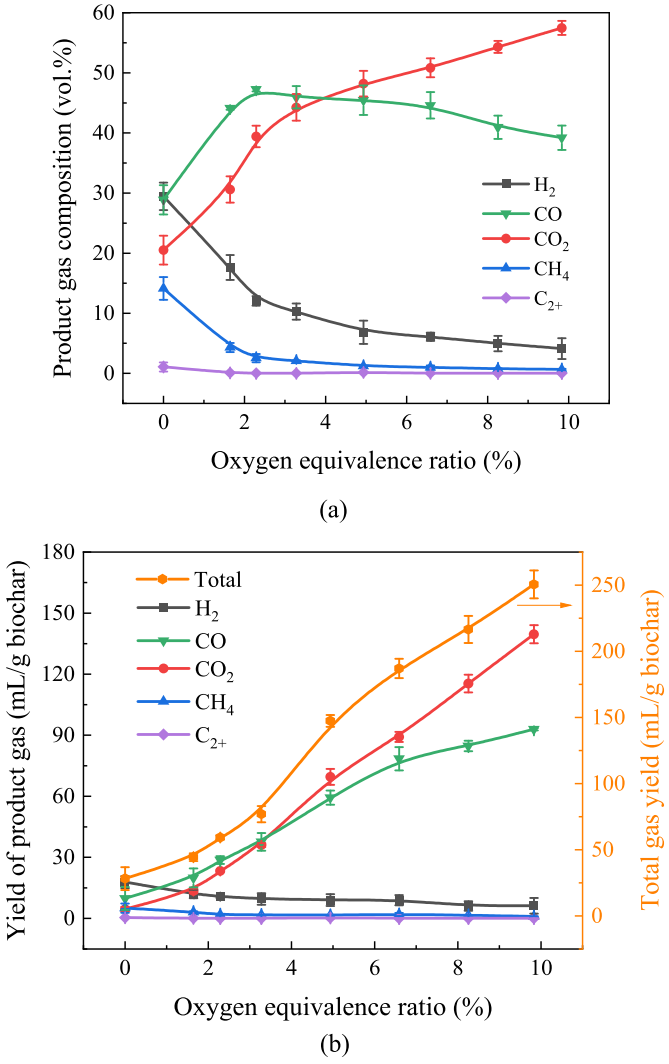

Fig. 3. Composition and volumetric yield of product gas from biochar oxidation in a fluidized-bed reactor under varying oxygen ERs at 600 °C: (a) gas composition, (b) gas yields.

3.3. Physiochemical structures of biochar before and after oxidation under lower ERs

3.3.1. Elemental composition of biochar

The elemental composition of biochar before and after oxidation in a fluidized-bed reactor under different ERs at 600 °C was analyzed and the

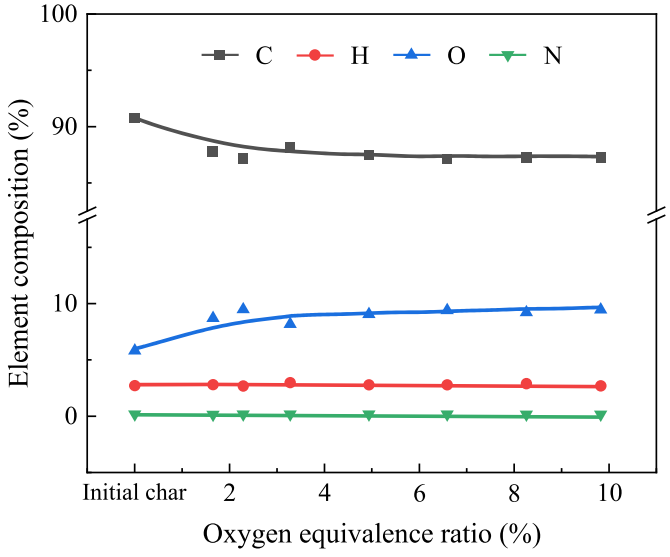

Fig. 4. Elemental composition of biochar before and after oxidation at 600 °C in a fluidized-bed reactor under different oxygen ERs.

results are displayed in Fig. 4. It is evident that the oxidation of biochar was accompanied by the decrease in C and H contents and an increase in O content with very low N in biochar under low-concentration and lower ERs of oxygen. This was consistent with the foregoing results of gaseous products evolving, where the oxidation of biochar consumed the surface C and H, resulting in a decrease in H_2 yield and a large increase in CO and CO_2 yields in the product gas. Oxidation of biochar was normally accompanied by the adsorption of molecular oxygen on its surface as well as the oxidation of the surface structures, which may introduce some oxygen-containing functional groups on its surface, leading to an increase in its O content [28]. However, in general, the changes in the elemental composition of biochar became relatively smaller with the increase of oxygen ER, which suggested that the increase of oxygen ER tended to more consume the mass of biochar, but relatively less change its composition.

3.3.2. *Microporosity of biochar*

The microporous structure of the biochar before and after oxidation in a fluidized-bed reactor at 600 °C under different ERs was analyzed and the results are shown in Table 1 and Figs. 5 and 6. As can be seen from Table 1, the biochar already possessed a good pore structure before oxidation, the BET surface area and pore volume were relatively high, and most of the pores were micropores, with the t-plot micropore surface area and micropore volume accounting for about 80 %. After oxidation under relatively lower oxygen ERs, it can be found that the BET surface area and pore volume of biochar increased. The oxidative etching of biochar surface by oxygen molecules somehow increased the pore structure of biochar, resulting in the increase in the surface micropores, corresponding to the increases in the t-plot micropore surface area and micropore volume. This was in agreement with the conclusion of pore making on biochar surface by hot-air oxidation as reported in literature [34,35]. However, it should be also noted that the increase in BET surface area and pore volume was not that significant as expected during biochar oxidation under oxidative pyrolysis conditions. This might be attributed to the well-developed pore structures of the initial char. The relatively high char preparation temperature (600 °C) and long preparation time (30 min) allowed for the sufficient removal of volatiles and the well-developed pore structures. The oxidative etching although was able to introduce a certain amount of micropores on the biochar surface, the improvement would not that significant. This might be somewhat different from the oxidative fast pyrolysis of biomass, where the pore structure of biochar was generally not sufficiently opened/developed within limited reaction time, whereas oxidative etching of biochar under oxidative pyrolysis conditions might improve its pore structure more remarkably.

The adsorption-desorption curves shown in Fig. 5 further confirmed that the pores in biochar were dominated by micropores, as a rapid increase in adsorption was observed at lower partial pressures ($P/P_0 < 0.1$). After introduction of oxygen, the micropore structure was significantly enhanced, whereas the effect of different oxygen ERs was insignificant. Fig. 6 further shows the variation of pore size distribution of biochar before and after oxidation at 600 °C under different ERs. From the figure, it can be seen that the pores of biochar were dominated by micro- and meso-pores [35], mainly in the range of 0.5–3 nm. After oxidation under low oxygen ERs, a significant increase in the micropores (below 2 nm) could be clearly seen for the biochar, further confirming that the oxidative etching of biochar surface by oxygen molecules mainly formed micropores, which was consistent with the previous results in Table 1 and Fig. 5.

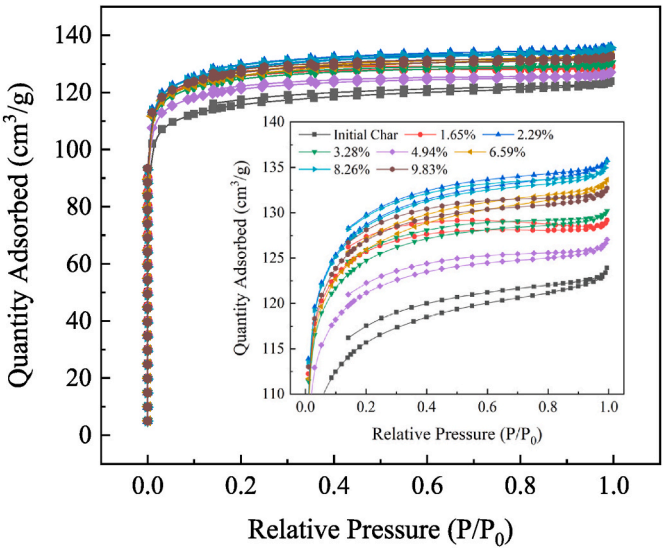

Fig. 5. Adsorption-desorption curves of biochar before and after oxidation at 600 °C under different oxygen ERs.

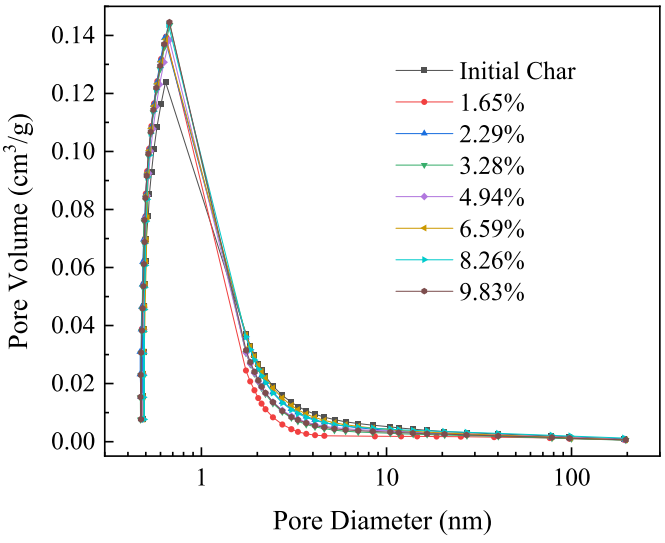

Fig. 6. Pore size distribution of biochar before and after oxidation at 600 °C under different oxygen ERs.

Table 1
Microporosity of biochar before and after oxidation at 600 °C under different oxygen ERs.

Biochar samples	BET Surface Area (m2/g)	t-Plot Micropore Surface Area (m2/g)	t-Plot External Surface Area (m2/g)	Pore Volume (× 10-2 cm3/g)	t-Plot Micropore Volume (× 10-2 cm3/g)	t-Plot External Volume (× 10-2 cm3/g)	Mean pore size (nm)
Initial char	350.67	282.77	67.90	19.17	14.92	4.25	2.19
1.65 %	379.10	322.15	56.95	19.98	16.95	3.03	2.11
2.29 %	389.49	319.37	70.11	21.02	16.83	4.18	2.16
3.28 %	376.94	314.00	62.95	20.14	16.53	3.61	2.14
4.94 %	366.26	304.46	61.79	19.65	16.04	3.62	2.15
6.59 %	381.67	312.84	68.84	20.68	16.46	4.21	2.17
8.26 %	389.17	318.00	71.17	20.98	16.76	4.23	2.16
9.83 %	383.79	318.69	65.10	20.53	16.79	3.74	2.14

3.3.3. Surface functional groups of biochar

Fig. 7 shows the FTIR spectra (4000-400 cm^{-1}) of biochar before and after oxidation at 600 °C under different oxygen ERs. As can be seen from the figure, the surface functional groups detected on the biochar surface mainly included aromatic C-H, phenolic C-OH, aromatic C=C, carboxyl -COO, aliphatic C-H and hydroxy -OH [36,37]. The distribution of surface functional groups on biochar before and after oxidation was quite similar, only the peak intensities were different. It indicated that the types of surface functional groups of biochar did not change much before and after oxidation, while their relative contents altered. Compared to the initial char, the oxygen-containing functional groups (e.g., -OH, -COO and phenolic C-OH) on the biochar surface increased significantly after oxidation in a low-concentration of oxygen (ER). The chemisorption of oxygen molecules on biochar surface and the subsequent oxidation formed more oxygen-containing functional groups, especially the hydroxyl -OH group showing the most significant increase. With the increase of ER, the oxidation degree of biochar increased, the surface functional groups on biochar firstly increased and then decreased. The mild oxidation of biochar was observed to activate the surface of biochar, resulting in an increase in active functional groups/active sites on its surface. The -OH content got a maximal value at an ER of 3.28 %, while the contents of -COO, phenolic C-OH, aromatic C=C, and C-H reached the maximal levels at an ER of 6.59 %. The introduction of oxygen preferentially oxidized the more active amorphous carbon (defects) on the biochar surface, which somewhat led to an increase in the aromaticity of biochar, corresponding to the elevation in the contents of aromatic C=C and C-H and phenolic C-OH (Fig. 7). Further increasing ER (>6.59 %) would over intensify the oxidation of biochar, resulting in partial oxidation consumption of the above-mentioned functional groups by the incremental oxygen. In addition, the aliphatic C-H content was observed to decrease with ER increasing, which was consistent with the aforementioned results of gas evolving depicted in Fig. 3(a) and (b). Overall, it can be concluded that during oxidative pyrolysis of biomass or biochar oxidation under oxidative pyrolysis conditions, a suitable biochar surface chemical structure can be obtained by optimizing the oxygen ER or concentration used during the process.

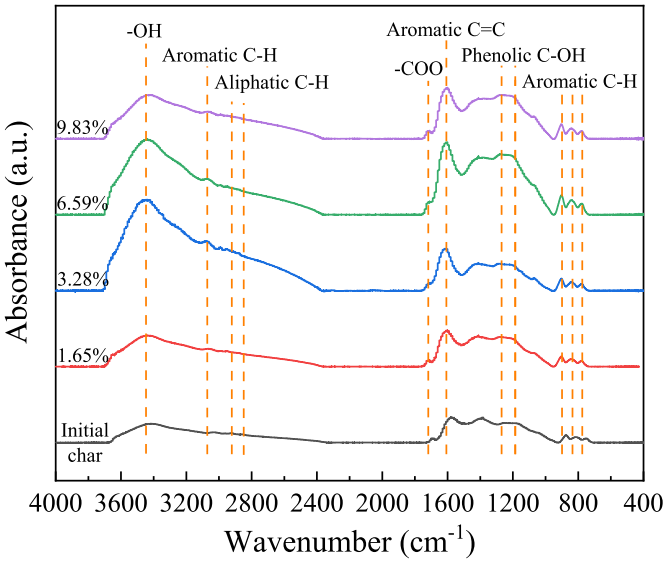

Fig. 7. FTIR spectra of biochar before and after oxidation at 600 °C under different oxygen ERs.

4. Conclusion

The effect of oxygen ER on biochar oxidation characteristics was investigated under oxidative pyrolysis conditions in a quartz-tube fluidized-bed reactor. It was found that under low ERs at 600 °C, two competing oxidation reactions were existed between biochar and oxygen to respectively form CO and CO_2, resulted in insignificant changes in the biochar oxidation consumption with ER increasing in the range of 1.65–4.94 %. When ER was below 2.29 %, the contents of CO and CO_2 both increased rapidly. Further increasing ER resulted in more CO_2 formation from biochar oxidation, which was favorable for reducing the biochar oxidation consumption and releasing more heat during oxidative pyrolysis of biomass. At an ER of 4.94 %, the content of CO_2 in the product gas exceeded that of CO. The oxidation of biochar under low-concentration or lower ER of oxygen tended to consume more combustible C and H in biochar, while the O content increased. The oxidative etching of biochar was also observed to introduce more micropores on the biochar surface and changed its surface chemical structures to form more oxygen-containing functional groups. The hydroxy (-OH) group on biochar surface increased significantly, and the aromatization degree of biochar also increased. The results reported in the study show the prospect to directly obtain optimized structures of active biochar from oxidative pyrolysis of biomass by simply adjusting the oxygen concentration/ER.

CRediT authorship contribution statement

Tianyu Lu: Writing – original draft, Investigation, Formal analysis, Data curation. **Dan Lin:** Writing – review & editing, Formal analysis. **Yusuf Makarfi Isa:** Writing – review & editing. **Alexander Kozlov:** Writing – review & editing. **Maxim Penzik:** Writing – review & editing. **Xing Xie:** Writing – review & editing, Supervision, Formal analysis. **Shihong Zhang:** Writing – review & editing, Supervision. **Haiping Yang:** Writing – review & editing, Supervision. **Bin Li:** Writing – review & editing, Supervision, Methodology, Funding acquisition, Conceptualization.

Declaration of competing interest

The authors declare that they have no known competing financial interests or personal relationships that could have appeared to influence the work reported in this paper.

Acknowledgements

The authors would like to express their sincere thanks for the financial supports from the National Natural Science Foundation of China (52276196), the Foundation of State Key Laboratory of Coal Combustion (FSKLCCA2508), and the High-level Talent Foundation of Anhui Agricultural University (rc412307).

References

[1] X. Tan, T. Tan, Biofuels from biomass toward a net-zero carbon and sustainable world, Joule 6 (2022) 1396–1399.
[2] S. Zhang, K. Zou, B. Li, H. Shim, Y. Huang, Key considerations on the industrial application of lignocellulosic biomass pyrolysis toward carbon neutrality, Engineering 29 (2023) 35–38.
[3] B. Li, X. Xie, L. Zhang, D. Lin, S. Wang, S. Wang, H. Xu, J. Wang, Y. Huang, S. Zhang, D. Liu, Coke formation during rapid quenching of volatile vapors from fast pyrolysis of cellulose, Fuel 306 (2021) 121658.
[4] D.E. Daugaard, R.C. Brown, Enthalpy for pyrolysis for several types of biomass, Energy & Fuels 17 (2003) 934–939.
[5] B. Li, J. Tang, X. Xie, J. Wei, D. Xu, L. Shi, K. Ding, S. Zhang, X. Hu, S. Zhang, D. Liu, Char structure evolution during molten salt pyrolysis of biomass: effect of temperature, Fuel 331 (2023) 125747.
[6] J.P. Polin, C.A. Peterson, L.E. Whitmer, R.G. Smith, R.C. Brown, Process intensification of biomass fast pyrolysis through autothermal operation of a fluidized bed reactor, Appl. Energy 249 (2019) 276–285.
[7] J. Polin, H. Carr, L. Whitmer, R. Smith, R. Brown, Conventional and autothermal pyrolysis of corn stover: overcoming the processing challenges of high-ash agricultural residues, J. Anal. Appl. Pyrol. 143 (2019) 104679.
[8] R.C. Brown, Heterodoxy in fast pyrolysis of biomass, Energy & Fuels 35 (2020) 987–1010.

[9] Y. Huang, B. Li, D. Liu, X. Xie, H. Zhang, H. Sun, X. Hu, S. Zhang, Fundamental advances in biomass autothermal/oxidative pyrolysis: a review, ACS Sustain. Chem. Eng. 8 (2020) 11888–11905.
[10] B. Li, M. Song, X. Xie, J. Wei, D. Xu, K. Ding, Y. Huang, S. Zhang, X. Hu, S. Zhang, D. Liu, Oxidative fast pyrolysis of biomass in a quartz tube fluidized bed reactor: effect of oxygen equivalence ratio, Energy 270 (2023) 126987.
[11] S. Zhao, Y. Luo, Y. Su, Y. Zhang, Y. Long, Experimental investigation of the oxidative pyrolysis mechanism of pinewood on a fixed-bed reactor, Energy & Fuels 28 (2014) 5049–5056.
[12] K.H. Kim, R.C. Brown, X.L. Bai, Partial oxidative pyrolysis of acid infused red oak using a fluidized bed reactor to produce sugar rich bio-oil, Fuel 130 (2014) 135–141.
[13] M. Amutio, G. Lopez, R. Aguado, J. Bilbao, M. Olazar, Biomass oxidative flash pyrolysis: autothermal operation, yields and product properties, Energy & Fuels 26 (2012) 1353–1362.
[14] G. Gao, X. Hu, Y. Shao, C. Li, L. Zhang, W. Gao, K. Ding, Y. Huang, M. Gholizadeh, S. Zhang, Influence of O2 on structural evolution of biochar in oxidative pyrolysis of cellulose, J. Anal. Appl. Pyrol. 181 (2024) 106576.
[15] G. Gao, S. Zhang, A. Gao, C. Li, L. Zhang, W. Gao, K. Ding, Y. Huang, M. Gholizadeh, X. Hu, Oxidative pyrolysis of poplar sawdust: probing the influence of oxidation reactions on property of biochar, J. Energy Inst. 115 (2024) 101624.
[16] G. Gao, S. Zhang, Y. Shao, C. Li, L. Zhang, W. Gao, K. Ding, Y. Huang, M. Gholizadeh, X. Hu, Oxidative pyrolysis of spirulina: impacts of oxygen on bio-oil and property of biochar, J. Environ. Chem. Eng. 12 (2024) 112506.
[17] W. Fu, X.W. Bai, Y. Tursun, Q. Liu, B. Li, Z.H. Dai, Y.P. Zhao, X. Li, L. Guo, J. Li, Oxidative pyrolysis of plywood waste: effect of oxygen concentration and other parameters on product yield and composition, J. Anal. Appl. Pyrol. 173 (2023) 106068.
[18] W.-J. Liu, H. Jiang, H.-Q. Yu, Development of biochar-based functional materials: toward a sustainable platform carbon material, Chem. Rev. 115 (2015) 12251–12285.
[19] F. Gan, B. Cheng, Z. Jin, Z. Dai, B. Wang, L. Yang, X. Jiang, Hierarchical porous biochar from plant-based biomass through selectively removing lignin carbon from biochar for enhanced removal of toluene, Chemosphere 279 (2021) 130514.
[20] H. Huang, Z. Niu, R. Shi, J. Tang, L. Lv, J. Wang, Y. Fan, Thermal oxidation activation of hydrochar for tetracycline adsorption: the role of oxygen concentration and temperature, Bioresour. Technol. 306 (2020) 123096.
[21] H. Wang, B.Z. Dlugogorski, E.M. Kennedy, Coal oxidation at low temperatures: oxygen consumption, oxidation products, reaction mechanism and kinetic modelling, Prog. Energy Combust. Sci. 29 (2003) 487–513.
[22] J.P. Polin, H.D. Carr, L.E. Whitmer, R.G. Smith, R.C. Brown, Conventional and autothermal pyrolysis of corn stover: overcoming the processing challenges of high-ash agricultural residues, J. Anal. Appl. Pyrol. 143 (2019) 104679.
[23] S. Zhao, Y. Zhang, Y. Su, Experimental investigation of rice straw oxidative pyrolysis process in a hot-rod reactor, J. Anal. Appl. Pyrol. 142 (2019) 104646.
[24] F. Xiao, A.H. Bedane, J.X. Zhao, M.D. Mann, J.J. Pignatello, Thermal air oxidation changes surface and adsorptive properties of black carbon (char/biochar), Sci. Total Environ. 618 (2018) 276–283.
[25] W. Suliman, J.B. Harsh, N.I. Abu-Lail, A.-M. Fortuna, I. Dallmeyer, M. Garcia-Perez, Modification of biochar surface by air oxidation: role of pyrolysis temperature, Biomass Bioenergy 85 (2016) 1–11.
[26] F. Xiao, A.H. Bedane, S. Mallula, P.C. Sasi, A. Alinezhad, D. Soli, Z.M. Hagen, M. D. Mann, Production of granular activated carbon by thermal air oxidation of biomass charcoal/biochar for water treatment in rural communities: a mechanistic investigation, Chemical Engineering Journal Advances 4 (2020) 100035.
[27] X. Zhu, C. Li, J. Li, B. Xie, J. Lü, Y. Li, Thermal treatment of biochar in the air/nitrogen atmosphere for developed mesoporosity and enhanced adsorption to tetracycline, Bioresour. Technol. 263 (2018) 475–482.
[28] B. Li, L. Zhao, X. Xie, D. Lin, H. Xu, S. Wang, Z. Xu, J. Wang, Y. Huang, S. Zhang, X. Hu, D. Liu, Volatile-char interactions during biomass pyrolysis: effect of char preparation temperature, Energy 215 (2021) 119189.
[29] C.F. Magoua Mbeugang, B. Li, D. Lin, X. Xie, S. Wang, S. Wang, S. Zhang, Y. Huang, D. Liu, Q. Wang, Hydrogen rich syngas production from sorption enhanced gasification of cellulose in the presence of calcium oxide, Energy 228 (2021) 120659.
[30] B. Li, C.F. Magoua Mbeugang, X. Xie, J. Wei, S. Zhang, L. Zhang, A.A. El Samahy, D. Xu, Q. Wang, S. Zhang, D. Liu, Catalysis/CO_2 sorption enhanced pyrolysis-gasification of biomass for H_2-rich gas production: effects of activated carbon, NiO active component and calcined dolomite, Fuel 334 (2023) 126842.
[31] K. Liu, Effects of sample size, dry ashing temperature and duration on determination of ash content in algae and other biomass, Algal Res. 40 (2019) 101486.
[32] Y. Zheng, J. Wang, D. Li, C. Liu, Y. Lu, X. Lin, Z. Zheng, Insight into the KOH/$KMnO_4$ activation mechanism of oxygen-enriched hierarchical porous biochar derived from biomass waste by in-situ pyrolysis for methylene blue enhanced adsorption, J. Anal. Appl. Pyrol. 158 (2021) 105269.
[33] J. Hu, Y. Si, H. Yang, J. Shao, X. Wang, T. Lei, F.A. Agblevor, H. Chen, Influence of volatiles-char interactions between coal and biomass on the volatiles released, resulting char structure and reactivity during co-pyrolysis, Energy Convers. Manag. 152 (2017) 229–238.
[34] F. Xiao, A review of biochar functionalized by thermal air oxidation, Environmental Functional Materials 1 (2022) 187–195.
[35] Z. Sun, L. Dai, P. Lai, F. Shen, F. Shen, W. Zhu, Air oxidation in surface engineering of biochar-based materials: a critical review, Carbon Research 1 (2022) 32.
[36] D. Feng, Y. Zhao, Y. Zhang, J. Gao, S. Sun, Changes of biochar physiochemical structures during tar H_2O and CO_2 heterogeneous reforming with biochar, Fuel Process. Technol. 165 (2017) 72–79.
[37] Y. Liu, M. Paskevicius, H. Wang, G. Parkinson, J.-P. Veder, X. Hu, C.-Z. Li, Role of O-containing functional groups in biochar during the catalytic steam reforming of tar using the biochar as a catalyst, Fuel 253 (2019) 441–448.